Comparison of the Hu-Duan Boundary Effect Model with the Size-Shape Effect Law for Quasi-Brittle Fracture Based on New Comprehensive Fracture Tests

Christian G. Hoover[1] and Zdeněk P. Bažant, Hon.M.ASCE[2]

Abstract: The boundary effect model (BEM) for concrete fracture and the effects of specimens size and crack length has previously been criticized on theoretical grounds, but the experimental evidence found in the literature, when taken alone, has been too limited to judge the validity of BEM conclusively. New, separately published, comprehensive fracture experiments, which were made on specimens cast from one and the same batch concrete and featured a broad ranges of both the size and the crack length (including a zero crack length), change the situation. The optimum fit of the data by Hu and Duan's model shows major deviations from these new test results. On the other hand, the Type 1 and 2 size effect laws (SELs) and their amalgamation in the universal size effect law are found to give a far better fit of the test results. Thus, regardless of the previously expounded theoretical objections, the comparison with experimental evidence alone suffices to conclude that Hu and Duan's model is not realistic. **DOI: 10.1061/(ASCE)EM.1943-7889.0000632.**

Author keywords: Cohesive crack; Scaling; Concrete; Asymptotics of fracture; Statistics of experimental data.

Introduction

Although a vast amount of test data on concrete fracture exists in the literature, the experimental verification of theoretical models has been hampered by the fact that most data sets have a rather limited range and have been obtained for different concretes and under different test conditions. It is thus not surprising that rather different theoretical models have happily coexisted for a long time, and polemics about their differences have not resulted in a universal consensus.

One such model that received much publicity is the boundary effect model (BEM). It was first proposed by Hu and Wittmann (2000) and subsequently elaborated on in a series of papers by Hu and Duan (Duan and Hu 2004; Duan et al. 2006; Hu 2002; Hu and Duan 2007, 2008, 2010). This model was critically examined in this journal in a recent paper by Yu et al. (2010). Significant theoretical objections were raised, but their experimental verification was incomplete because the test data available had a rather limited scope.

The situation has now changed with the publication (Hoover et al. 2013) of extensive experimental data on the structure size and crack length effects in notched and unnotched three-point bend beams cast from the same concrete. These data are comprehensive enough to check the basic hypothesis of Hu and Duan's model for the case of three-point bend beams (the data are summarized in a later section and used to compare the BEM with the size effect laws).

Review of Energetic Size Effect Laws of Types 1 and 2

Because Hu and Duan contrasted their recently proposed BEM with the size effect law (SEL) derived in 1984 (Bažant 1984) from energy release arguments and reformulated in 1991 (Bažant and Kazemi 1991) in terms of dimensionless energy release function $G(\alpha)$ of linear elastic fracture mechanics (LEFM), this law is summarized first. For Type 2 failures, which are those occurring when there is a notch or large stress-free crack formed before reaching the maximum (or ultimate) load P_u, this law reads

$$\sigma_N = \frac{Bf_t'}{\sqrt{1+D/D_0}} = \sqrt{\frac{E'G_f}{g(\alpha_0)D + g'(\alpha_0)c_f}} \tag{1}$$

where, for two-dimensional scaling, $\sigma_N = c_N P_u/bD$ = nominal strength of the structure; c_N = conveniently chosen dimensionless factor (often chosen as 1); D = size of structure; b = its width in the third dimension; f_t' = tensile strength; B = geometry dependent dimensionless constant; D_0 = constant called the transitional size; $\alpha = \alpha/D$ = relative crack length of notch or stress-free crack, $\alpha_0 = a_0/D_0$ = initial value of α; G_f = initial fracture energy, representing the area under the initial tangent of the bilinear softening stress-separation curve of cohesive (or fictitious) crack model; $g(\alpha) = k^2(\alpha)$ = dimensionless LEFM energy release curve; and $k(\alpha)$ = dimensionless stress intensity factor.

Eq. (1) is not valid for $\alpha \to 0$. This is the case of Type 1 size effect, which occurs for structural geometries (such as unnotched beams) for which the failure occurs as soon as a macrocrack initiates from a smooth surface. According to the cohesive crack model, the large-size asymptote (for $D \to \infty$) of the size effect plot of $\log \sigma_N$ versus $\log D$ must be horizontal when the statistical Weibull size effect (Weibull 1939, 1951) is negligible, which is the case for the three-point bend beams, and for $D \to 0$, there must be another horizontal asymptote. For small and medium sizes, the Type 1 size effect is a

[1]Postdoctoral Research Associate, Dept. of Civil and Environmental Engineering, Massachusetts Institute of Technology, Cambridge, MA 02139; formerly, Graduate Research Assistant, Dept. of Civil and Environmental Engineering, Northwestern Univ., 2145 Sheridan Rd., CEE/A135, Evanston, IL 60208.

[2]McCormick Institute Professor and W. P. Murphy Professor of Civil and Mechanical Engineering and Materials Science, Northwestern Univ., 2145 Sheridan Rd., CEE/A135, Evanston, IL 60208 (corresponding author). E-mail: z-bazant@northwestern.edu

Note. This manuscript was submitted on August 16, 2012; approved on March 18, 2013; published online on February 14, 2014. Discussion period open until August 1, 2014; separate discussions must be submitted for individual papers. This paper is part of the ***Journal of Engineering Mechanics***, Vol. 140, No. 3, March 1, 2014. ©ASCE, ISSN 0733-9399/2014/3-480–486/$25.00.

smooth transition between these two asymptotes expressed (without the Weibull component) as follows (Bažant 2005):

$$\sigma_N = f_{r,\infty}\left(1 + \frac{rD_b}{D + l_p}\right)^{1/r} \tag{2}$$

Here, $f_{r,\infty}$, D_b, l_p, and r = constants of the model whose values need to be determined empirically; D_b = depth of the boundary layer of cracking [about equal to the fracture process zone (FPZ) width]; $f_{r,\infty}$ = nominal strength for very large structures (assuming negligible Weibull statistical size effects); and l_p = material characteristic length that is related to the maximum aggregate size. The initial asymptote is an abstraction that makes it possible to match the predictions of the cohesive crack model and thus provides a plastic upper bound on σ_N.

A smooth transition between the Type 1 and Type 2 size effects is described by the universal SEL (USEL), whose improved version was formulated and validated in the companion paper (Hoover and Bažant 2014).

Review of Hu and Duan's Model

Hu and Duan's BEM is based on a hypothesis about the effect of crack length on the nominal strength σ_N of a fracture specimen, illustrated by Fig. 1 and described by the following equation:

$$\sigma_N = \frac{f_t'}{\sqrt{1 + a_0/a_{\mathrm{FPZ}}}} \tag{3}$$

Here a_0 = length of the initial crack (or initial notch) without considering the FPZ; $a_{\mathrm{FPZ}} = l_{CH}/1.12^2\ \pi \approx 0.25 l_{CH}$; $l_{CH} = (K_{IC}/f_t')^2 = E'G_F/f_t'^2$ = Irwin's (1958) critical (or characteristic) length based on the total fracture energy G_F (Hillerborg et al. 1976; Hillerborg 1985); K_{IC} = critical K_I (or fracture toughness); K_I = mode I stress intensity factor; $E' = E$ for plane stress and $E' = E/(1 - \nu^2)$ for plane strain; E = Young's modulus; and ν = Poisson ratio.

The BEM and the Type 2 SEL differ in the definition of the fracture energy that they use. Whereas the SEL corresponds to the area under the initial tangent of the softening bilinear stress-separation curve of the cohesive crack model, which represents the initial fracture energy G_f (and can be used to determine G_f from size effect tests), Hu and Duan's BEM uses the total area under the softening curve, which represents the total fracture energy G_F (Hu and Wittmann 2000; Duan et al. 2006).

Aiming to capture not only the crack length effect but also the effect of structure size on the nominal strength of geometrically similar structures, Hu and Duan (2007, 2008) had to introduce the following modification of Eq. (3):

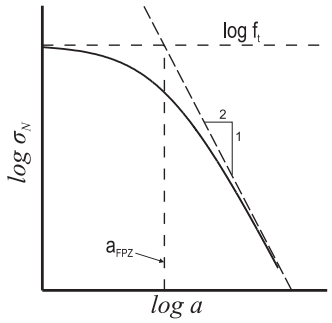

Fig. 1. Dependence of σ_N on crack length in concrete assumed by Hu and Duan BEM (cf., e.g., Fig. 2 in Hu and Duan 2010)

$$\sigma_N = \frac{A(\alpha)f_t'}{\sqrt{1 + W/W^*}} = \frac{A(\alpha)f_t'}{\sqrt{1 + W\alpha B(\alpha)/a_{\mathrm{FPZ}}}} \tag{4}$$

in which $W = D$ = depth of the beam; $\alpha = a_0/W$; and $B(\alpha) = [A(\alpha)\mathrm{Y}(\alpha)/1.12]^2$. $A(\alpha)$ is a factor relating the fictitious stress σ_n at the notch tip calculated under the assumption of a linear stress profile (i.e., ignoring the elastic stress singularity) to the nominal stress σ_N defined as the stress at the tensile face of unnotched beam calculated according to the beam theory (in which case $C_N = 3L/2D$, L = span).

In three-point bending (TPB), $\sigma_N = A(\alpha)\sigma_n = (1 - \alpha)^2\sigma_n$. Eq. (4) then becomes

$$\sigma_N = \frac{(1 - \alpha)^2 f_t'}{\sqrt{1 + D\alpha\pi[Y(\alpha)]^2(1 - \alpha)^4 f_t'^2/EG_F}} \tag{5}$$

(however, as shown later, the fit of the size effect data for $\alpha \to 0$ is poor). Based on Tada et al. (1985) and ASTM (1990), Hu and Duan also introduced the geometry factor

$$Y(\alpha) = \frac{1.99 - \alpha(1 - \alpha)\left(2.15 - 3.93\alpha + 2.7\alpha^2\right)}{\sqrt{\pi}\,(1 + 2\alpha)(1 - \alpha)^{3/2}} \tag{6}$$

Review of Comprehensive Tests of Size and Crack Length Effects

The experimental data published in a previous paper by Hoover et al. (2013) and also described in Hoover and Bažant (2013, 2014) are sufficiently extensive and systematic to assess the validity of Hu and Duan's BEM [Eqs. (3)–(5)]. All the specimens were cast from the same batch of concrete. They were geometrically similar three-point bend beams of four different depths, $D = 500, 215, 93$ and 40 mm, and five different relative crack lengths, $a_0/D = 0, 0.025, 0.075, 0.15$ and 0.30 for each size, except that the notch $a_0/D = 0.025$ was skipped for the two smallest sizes (because it would have been much shorter than the coarse aggregate diameter d_a and thus essentially equivalent to the case $\alpha = a/D = 0$).

The Type 2 SEL was fitted to the means of each family of tests for $\alpha = 0.30$ and 0.15. The means for each family are shown as large and thin x-points (Figs. 2 and 3). Hu and Duan's Eq. (4) also fits these data quite well, but only if f_t' and a_{FPZ} are optimized. This is expected because Eq. (4) has the same form as the Type 2 SEL. For $\alpha = 0.075$, the BEM also fits the data quite well; however, the Type 2 SEL is not applicable for $\alpha < 0.1$, and the USEL needs to be used instead (Hoover and Bažant 2014). The parameters for the optimal fits are listed in Table 1 (where G_F from the BEM is calculated from a_{FPZ}).

For the same notch depth, the values of tensile strength f_t' given in Tables 1 and 2 are different. The reason is that the data are optimally fitted by the BEM in two different ways. The first is to fit the BEM [Eq. (4)] to the comprehensive size effect data assuming that f_t' and a_{FPZ} are not known. The second is to use Eq. (5), along with the average total fracture energy G_F calculated by the Hillerborg (or work-of-fracture) method from the diagrams of load versus load-point displacement, to find the optimal values of f_t' for each data set, as discussed in the next section.

G_F was determined using the work-of-fracture method (Hoover and Bažant 2013) or Hillerborg's model (Shah 1990; RILEM 1985), in which one calculates the area under the load versus the load-point displacement curve, applies a correction for the self-weight of the beam, and divides the result by the ligament area (Table 1). The G_F value from the BEM is about half that calculated from the work-of-fracture method, which is a significant deficiency.

J. Eng. Mech. 2014.140:480-486.

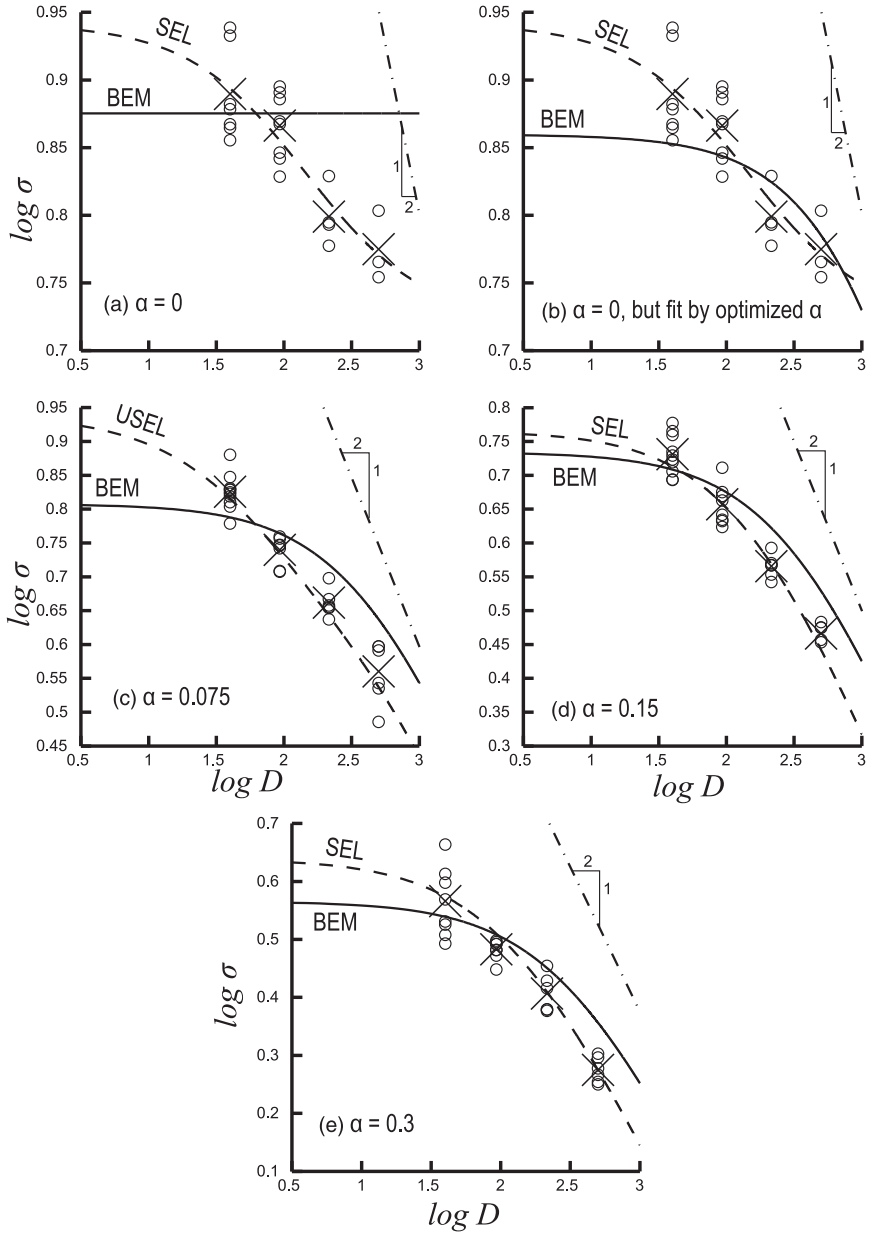

Fig. 2. BEM size effect trends: open circles are individual data points, solid lines represent BEM [Eq. (5)] fitted with the same material parameters to the entire data set, and dashed lines are the optimum fits by the SEL; (a) $\alpha = 0$; (b) $\alpha = 0$, but fit by optimized α; (c) $\alpha = 0.075$; (d) $\alpha = 0.15$; (e) $\alpha = 0.3$

The tensile strength f_t' can also be calculated from the initial fracture energy G_f and corresponding Irwin's relation $l_{ch} = E'G_f/f_t'^2$; l_{ch} is related to the effective length of fracture process zone c_f by $l_{ch} = c_f/\gamma$ (Cusatis and Schauffert 2009), where $\gamma = 0.29$ (Cusatis and Schauffert 2009) or $\gamma = 0.28$ (Yu et al. 2010). The initial fracture energies G_f for $\alpha = 0.30$ and $\alpha = 0.15$ (Hoover and Bažant 2013), as well as the respective c_f-values, yield the tensile strengths listed in Table 1. It is clear that the BEM gives values of G_F that are significantly lower (about half) than the widely accepted work-of-fracture method. The BEM also overestimates f_t' by more than 50%. These are again significant deficiencies.

Comparison of Optimum Fits of Size Effect Data by BEM and SEL

The optimal fits with the BEM and SEL are shown in Figs. 2 and 3 by the solid and dashed lines, respectively. The open circles in Fig. 2 represent the individual tests, and the means of each group of points are marked by thin but large x points. Including the individual data points gives a clear impression of the magnitude of scatter, but the visual comparison with the data means is cluttered. Therefore, to make the comparisons with the mean results conspicuous, the data means from the group for each size D are replotted in Fig. 3.

The BEM and SEL fits are optimized in Figs. 2 and 3 with the restriction that all the material parameters of each model be the same for all tests. The optimization is carried out with the least-square Levenberg-Marquardt optimization algorithm. The BEM was fitted to the entire data set simultaneously. The optimized f_t' for the entire data set is 7.3 MPa, and the coefficients of variation (COV; defined as the RMS error divided by the mean of all data) for the BEM are listed in Table 2. The average G_F from $\alpha = 0.3$ and $\alpha = 0.15$ equal to 104 N/m was used. The BEM was also fitted to each individual set for comparison. The optimized f_t and the COV of fit for each graph

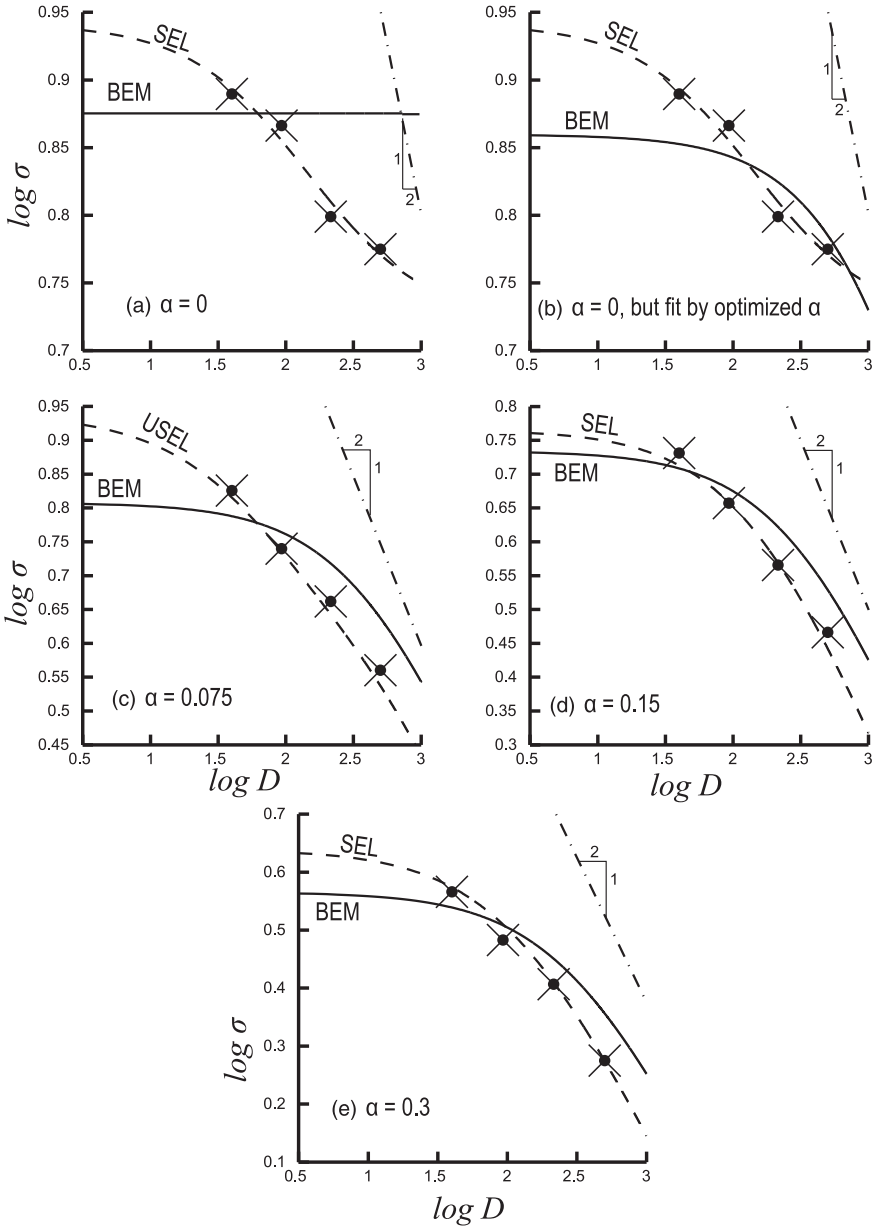

Fig. 3. BEM size effect trends: solid lines are BEM [Eq. (5)] fitted with the same material parameters to the entire data set, and dashed lines are the optimum fits by the SEL; (a) $\alpha = 0$; (b) $\alpha = 0$, but fit by optimized α; (c) $\alpha = 0.075$; (d) $\alpha = 0.15$; (e) $\alpha = 0.3$

Table 1. Optimum Value of f_t' and a_{FPZ} from BEM for Each Relative Notch Length α from Eq. (4)

α[a]	0.3	0.15	0.075
a_{FPZ} (mm)	7.66	8.3	6.34
G_F (N/m) (from BEM)	53.4	55.4	45.8
G_F (N/m) (from Hoover and Bažant 2013)	96.9	110.5	—
c_f (from Hoover and Bažant 2013)	27.97	20.99	—
f_t' (MPa) (from BEM)	8.52	8.34	8.67
f_t' (MPa) (from c_f)	4.63	5.23	—

[a]$\alpha = 0.3$, 0.15, and 0.075, respectively.

in Figs. 2 and 3 are also provided in Table 2, along with the COV of fit for the size effect laws.

The optimum material properties used in the Type 2 SEL were $G_f = 49.56\,(\mathrm{N/m})$ and $c_f = 22.34\,(\mathrm{mm})$, determined by fitting Eq. (2) simultaneously to the $\alpha = 0.3$ and $\alpha = 0.15$ beams. This gives $f_t' = 5.07\,\mathrm{MPa}$. The optimum material parameters used in fitting the crack initiation specimens were $D_b = 73.2\,\mathrm{mm}$, $l_p = 126.6\,\mathrm{mm}$, $f_{r,\infty} = 5.27\,\mathrm{MPa}$, and $r = 0.52$. The parameters used in the universal size effect law are discussed in Hoover and Bažant (2014).

As seen in Figs. 2 and 3, for deep notches ($\alpha = 0.30$ and 0.15), the size effect fits by BEM are worse than those by SEL, and for short or zero notches, they are much worse. For $\alpha = 0$, the Type 1 SEL agrees with the data points quite well. Also, it shows a double curvature, which agrees with the fact that, according to the cohesive crack model, the curve should approach two horizontal asymptotes: one for small sizes and one for large sizes.

J. Eng. Mech. 2014.140:480-486.

At $\alpha = 0$, the plot of the BEM size effect in Figs. 2 and 3 is a horizontal line, i.e., no size effect is predicted [Figs. 2(a) and 3(a)], This is a problem for the simple BEM. To circumvent it, Hu and Duan proposed that, in absence of a notch, one needs to consider that there must exist a pre-existing equivalent crack corresponding to a certain finite $\alpha = \alpha_{eq} = a_{eq}/D$. However, this artifice is theoretically objectionable (Yu et al. 2010).

The main reason is that, while optimizing α_{eq}, it is implied that the size of the largest flaw is assumed to be proportional to the structure size D (i.e., as D increases, the largest flaw size a increases). However, this assumption is flawed. If the size of the largest flaw in a 10-cm-deep test beam is 1 cm, one would have to infer that the size of inevitable flaws in the 6-m-deep unreinforced plinth of the failed Schoharie Creek Bridge would reach 0.6 m. That agrees neither with observations nor with statistics. The flaw size distribution is strictly a material property and thus cannot be a function of the structure size (nor shape).

Nevertheless, let us check what is implied. Because the value of this equivalent α is unclear, the α_{eq} value that should replace $\alpha = 0$ has been optimized. The optimization ensures that no other α value can give for a notchless specimen a better BEM prediction.

Table 2. Comparison of f_t' and Size Effect, COV of Curve Fits

Figures	COV (%)[a]	f_t' (MPa)[b]	COV (%)[b]	COV (%)[c]
Fig. 3(a)	12.7	—	—	1.91
Fig. 3(b)	7.21	8.55	3.56	1.91
Fig. 3(c)	12.8	7.08	12.6	3.15
Fig. 3(d)	12.3	6.92	11.5	2.58
Fig. 3(e)	11.5	7.08	11.3	2.54

[a]Determined from fitting Eq. (5) to the entire data set at once.
[b]Determined from fitting Eq. (5) to each individual geometry.
[c]Determined from fitting the SELs.

The corresponding optimum fit with BEM is shown by the solid curve in Figs. 2(b) and 3(b), for which $\alpha_{eq} = 0.015$. This value was optimized along with f_t' for the entire collection of data. Eq. (5) can also be fitted to the collection of notchless beams alone, for which the optimized $\alpha_{eq} = 0.039$. Figs. 2(c) and 3(c) also display, for comparison, the optimum fit of the $\alpha = 0.075$ beams according to the USEL. This law, which was presented (in an improved form) in the companion paper (Hoover and Bažant 2014), gives a formula for a smooth transition between the size effects of Types 1 and 2. Again, the fit by the BEM, even though artificially adjusted for $\alpha = 0$, is seen to be inferior.

The f_t value obtained when $\alpha = \alpha_{eq}$ is about 18% higher than the other f_t values. This shows that the BEM cannot predict the strength of beams with notches if it is fitted to specimens with no notch. It also demonstrates that the BEM cannot predict the strength of beams when $\alpha = 0$ if it is first calibrated to notched test specimens.

Table 2 also compares the tensile strength f_t', and COVs of the BEM and SEL. In all cases, the SEL fits are distinctly more accurate. The BEM also gives f_t' values that are about 40% higher than those determined from the SEL (Table 2).

Comparisons in Terms of Crack Length Effect

Eq. (5) of the BEM was originally proposed for the crack length effect on σ_N. Figs. 4 and 5 show by solid curves the optimum BEM fit of the observed relative crack (notch) length effect for four specimen sizes D, compared, respectively, with the individual data

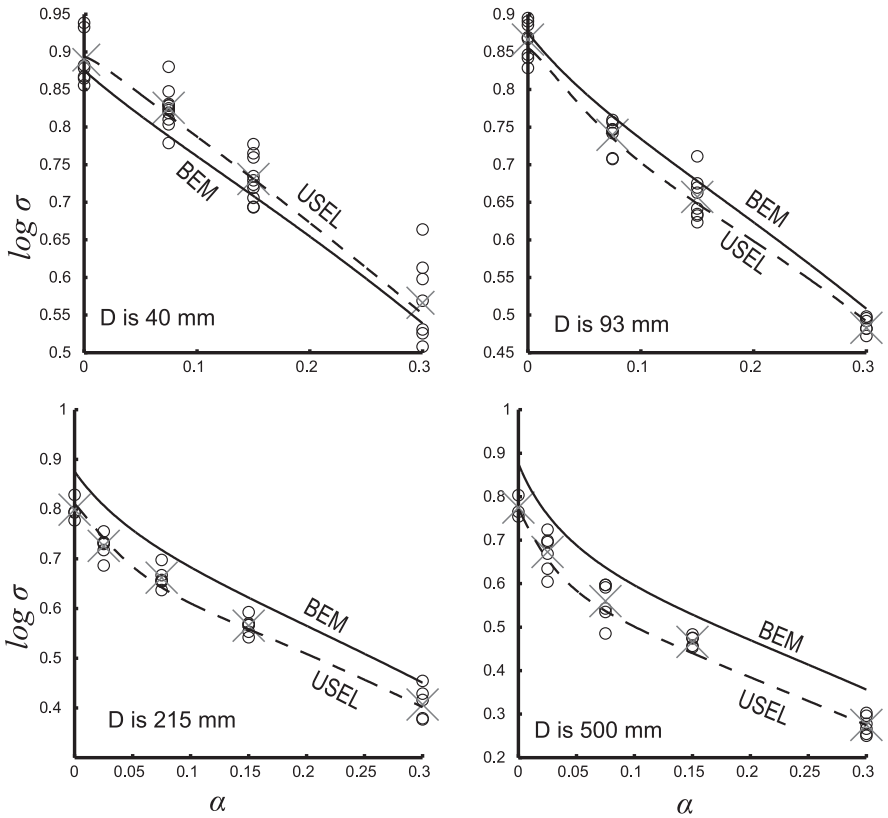

Fig. 4. Effect of relative crack length α on the nominal strength σ_N optimally fitted by BEM using the same material parameters, shown by solid lines, and by the SEL (with the Type 1–Type 2 transition), shown by dashed lines: open circles are the individual test data points; BEM crack length effect trends; the solid lines represent [Eq. (5)] fit to the whole data set, and the dashed curve represents the fit by the USEL [Eq. (1)]

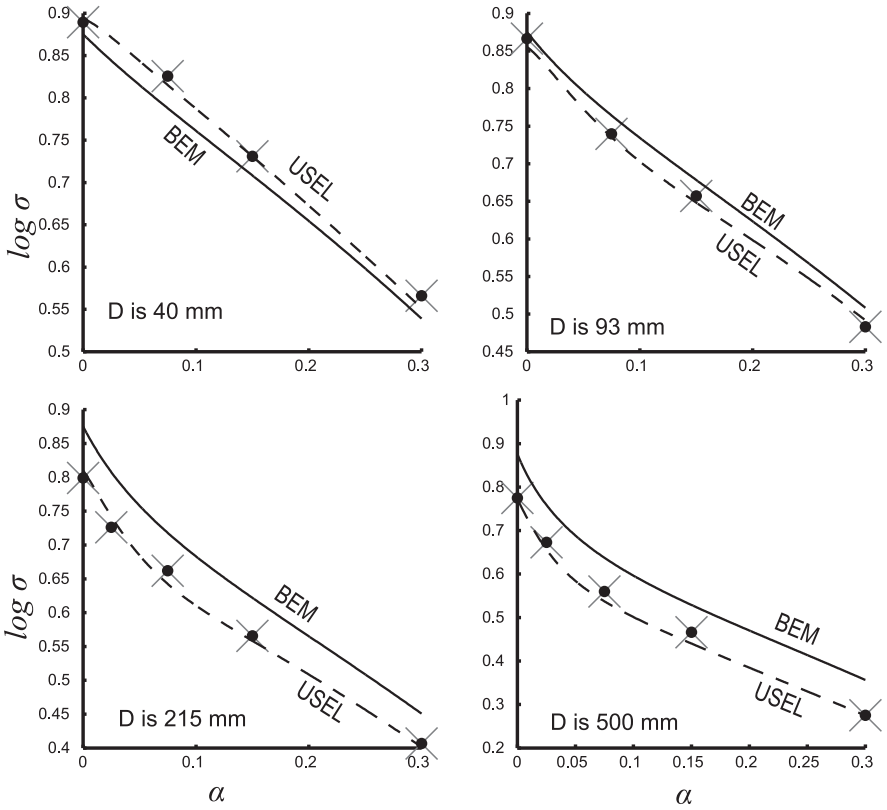

Fig. 5. Effect of relative crack length α on the nominal strength σ_N optimally fitted by BEM using the same material parameters, shown by solid lines, and by the SEL (with the Type 1–Type 2 transition), shown by dashed lines: BEM crack length effect trends; the solid lines represent [Eq. (5)] fit to the whole data set, and the dashed curve represents the fit by the USEL

points and to the mean values for each α considered. The optimized material parameters for this fit are the same as was used for the size effect plots.

Figs. 4 and 5 also shows the optimum fit of the crack length effect using the USEL from Hoover and Bažant (2014), which is equivalent to the simple Type 2 SEL [Eq. (1)] when $\alpha \geq 0.15$ and to the Type 1 SEL when α vanishes (i.e., when there is no notch). In this case the optimized material parameters are $G_f = 56.25$ N/m, $c_f = 29.79$ mm, and $f_t' = 4.68$ MPa (Hoover and Bažant 2014). The comparison again shows that the BEM is distinctly inferior. The COV of fit for each graph in Figs. 4 and 5 is provided in Table 3.

When $\alpha \to 0$, the strength for all sizes D approaches the same value. This is consistent with the BEM graph in Figs. 2 and 3, but is in conflict with the experimental data on the Type 1 size effect and the Type 1 SEL.

Another point to note is that the optimized equivalent relative notch length α_{eq} needed to match the strength of notchless specimens ($\alpha = 0$) is constant (Hu and Duan 2010), which implies that the initial notch length a_{eq} varies with structure size. However, it is claimed in Hu and Duan (2010) that a_{eq} is supposed to be a material property on the order of aggregate size. So why should the length a of the preexisting cracks vary with structure size? This implication is not realistic.

It has been noted that the BEM fit of the crack length effect could be improved if the f_t' and G_f were optimized to fit this effect only. However, other problems would arise, e.g., excessive f_t', especially for $\alpha \to 0$, and a fracture energy G_F, which is about 50% less than calculated from the work-of-fracture method. It has also been noticed that if G_F in the BEM were replaced with G_f, then the fits in Figs. 2–5 would become somewhat better. However, they would still be significantly inferior to the SEL and USEL fits shown in these figures.

Table 3. Comparison of Crack Length Effect, COV of Curve Fits

Depth (mm)	COV (%)[a]	COV (%)[b]
40	7.9	2.03
93	3.92	2.32
215	17.1	2.91
500	23.9	2.5

[a]Determined from fitting Eq. (5) to the entire data set at once.
[b]Determined from fitting the USEL.

Conclusion

The new comprehensive fracture tests of concrete with broad size ranges of both the specimen size and the relative crack depth, including zero and very short depths, make it possible to examine Hu and Duan's BEM solely on the basis of experimental evidence. Although the BEM gives trends somewhat resembling the observations of the size effect and crack length effect in notched three-point bend beams, it gives a poor representation of the data from these new tests. In fitting these data, the BEM is distinctly inferior to the SELs, both Types 1 and 2, and their transition described by the universal SEL.

Acknowledgments

Financial support from the U.S. DOT, provided through Grant No. 20778 from the Infrastructure Technology Institute of Northwestern University, is gratefully appreciated.

References

ASTM. (1990). "Standard test method for plane-strain fracture toughness testing of high strength metallic materials." *ASTM E399-90*, West Conshohocken, PA.

Bažant, Z. P. (1984). "Size effect in blunt fracture: Concrete, rock, metal." *J. Eng. Mech.*, 10.1061/(ASCE)0733-9399(1984)110:4(518), 518–535.

Bažant, Z. P. (2005). *Scaling of structural strength*, Elsevier Butterworth-Heinemann, Burlington, MA.

Bažant, Z. P., and Kazemi, M. T. (1991). "Size dependence of concrete fracture energy determined by RILEM work-of-fracture method." *Int. J. Fract.*, 51(1), 121–138.

Cusatis, G., and Schauffert, E. (2009). "Cohesive crack analysis of size effect." *Eng. Fract. Mech.*, 76(14), 2163–2173.

Duan, K., and Hu, X. (2004). "Specimen boundary induced size effect on quasi-brittle fracture." *Strength Fract. Complexity*, 2(2), 47–68.

Duan, K., Hu, X., and Wittmann, F. (2006). "Scaling of quasi-brittle fracture: Boundary and size effect." *Mech. Mater.*, 38(1–2), 128–141.

Hillerborg, A. (1985). "The theoretical basis of a method to determine the fracture energy g_f of concrete." *Mater. Struct.*, 18(4), 291–296.

Hillerborg, A., Modeer, M., and Petersson, P. E. (1976). "Analysis of crack formation and crack growth in concrete by means of fracture mechanics and finite elements." *Cem. Concr. Res.*, 6(6), 773–782.

Hoover, C. G., and Bažant, Z. P. (2013). "Comprehensive concrete fracture tests: Size effects of types 1 and 2, crack length effect and postpeak." *Eng. Fract. Mech.*, 110, 281–289.

Hoover, C. G., and Bažant, Z. P. (2014). "Universal size-shape effect law based on comprehensive concrete fracture tests." *J. Eng. Mech.*. 10.1061/(ASCE)EM.1943-7889.0000627, 473–479.

Hoover, C. G., Bažant, Z. P., Vorel, J., Wendner, R., and Hubler, M. H. (2013). "Comprehensive concrete fracture tests: Description and results." *Eng. Fract. Mech.*, 114, 92–103.

Hu, X. (2002). "An asymptotic approach to size effect on fracture toughness and fracture energy of composites." *Eng. Fract. Mech.*, 69(5), 555–564.

Hu, X., and Duan, K. (2007). "Size effect: Influence of proximity of fracture process zone to specimen boundary." *Eng. Fract. Mech.*, 74(7), 1093–1100.

Hu, X., and Duan, K. (2008). "Size effect and quasi-brittle fracture: The role of FPZ." *Int. J. Fract.*, 154(1–2), 3–14.

Hu, X., and Duan, K. (2010). "Mechanism behind the size effect phenomenon." *J. Eng. Mech.*, 10.1061/(ASCE)EM.1943-7889.0000070, 60–68.

Hu, X., and Wittmann, F. (2000). "Size effect on toughness induced by crack close to free surface." *Eng. Fract. Mech.*, 65(2–3), 209–221.

Irwin, G. R. (1958). "Fracture." *Handbuch der physik*, S. Flgge, ed., Springer, Berlin, 551–590.

RILEM. (1985). "Determination of the fracture energy of mortar and concrete by means of three-point bend tests on notched beams." *Mater. Struct.*, 18(4), 285–290.

Shah, S. P. (1990). "Size-effect method for determining fracture energy and process zone size of concrete." *Mater. Struct.*, 23(6), 461–465.

Tada, H., Paris, P., and Irwin, G. (1985). *The stress analysis of cracks handbook*, 2nd Ed., Paris Productions, Hellerton, PA.

Weibull, W. (1939). "The phenomenon of rupture in solids." *Proc. R. Swedish Inst. Eng. Res.*, 153, 1–55.

Weibull, W. (1951). "A statistical distribution function of wide applicability." *J. Appl. Mech.*, 18, 293–297.

Yu, Q., Le, J. L., Hoover, C. G., and Bažant, Z. P. (2010). "Problems with Hu-Duan boundary effect model and its comparison to size-shape effect law for quasi-brittle fracture." *J. Eng. Mech.*, 10.1061/(ASCE)EM.1943-7889.89, 40–50.

J. Eng. Mech. 2014.140:480-486.